IEEE Access
Multidisciplinary | Rapid Review | Open Access Journal

Received May 8, 2017, accepted June 5, 2017, date of publication June 22, 2017, date of current version July 24, 2017.

Digital Object Identifier 10.1109/ACCESS.2017.2718558

Image Denoising Algorithm Based on Entropy and Adaptive Fractional Order Calculus Operator

JIMIN YU[1], LIJIAN TAN[1], SHANGBO ZHOU[2], LIPING WANG[2], AND MUHAMMAD ABUBAKAR SIDDIQUE[3]

[1]College of automation, Chongqing University of Posts and Telecommunications, Chongqing 400065, China
[2]Key Laboratory of Dependable Service Computing in Cyber Physical Society, Ministry of Education, Chongqing University, Chongqing 400044, China
[3]Khwaja Fareed University of Engineering and Information Technology, Rahim Yar Khan 62400, Pakistan

Corresponding author: Shangbo Zhou (shbzhou@cqu.edu.cn)

This work was supported in part by the Major Project of the Fundamental Science and Frontier Technology Research of Chongqing CSTC under Grant cstc2015jcyjBX0124, in part the National High-tech Research and Development Program of China under Grant 2015AA015308, and in part the Innovation Team Project of Chongqing Education Committee under Grant CXTDX201601019.

ABSTRACT In this paper, a fractional calculus operator for image denoising is constructed based on the characteristic of local entropy and the gradient feature, and an adaptive fractional calculus image denoising algorithm is proposed. First, the effects on the entropy and gradient by noise are analyzed, respectively. Second, the noise points are regarded as small probability events in an image, and the noise points, edges, texture regions, and smooth regions are divided combining with the local structure. Finally, for improving the image denoising effect, we consider employing different fractional orders to deal with different pixels and a piecewise function is constructed to make the differential order to be adaptive. The function is with respect to the local entropy and gradient on the pixel. The experimental results show that the peak signal-to-noise ratio and the entropy (ENTROPY) of the proposed adaptive fractional calculus image denoising algorithm are higher than that of the other algorithms compared in this paper. The proposed algorithm can not only preserve image edges and texture information while removing the noise, but also obtain a good visual effect.

INDEX TERMS Entropy, gradient, adaptive, fractional calculus, image denoising.

I. INTRODUCTION

At present, fractional calculus is rapidly developing in many fields of science and engineering. As a result, differential equations with arbitrary orders have been widely investigated for different applications in physics, fluid mechanics, physiology, engineering, potential theory and elasticity, etc [1]–[4]. In recent years, employing differential equation to image processing has become a hot research topic, and a large number of research results have been reported [5]–[12]. Compared with integer order calculus, fractional calculus method can enhance the edges and make the texture more clear while preserving the details information of smooth regions in the process of image denoising [13]. The traditional fractional calculus method employs the same order to deal with the image edges, texture and smooth regions. When a high fractional order is used to process the image noise, the weak texture and smooth regions will be ignored, for using a low fractional order, the image edges will be weakened. Therefore, the image denoising effect is not very good in practice by only using integer fractional calculus order. To cope with this problem, some combining with improved fractional calculus denoising algorithms are proposed.

Images are easy to be blurred by all kinds of noises in its proceeding of acquisition or transmission. Gaussian noise, impulse noise and speckle noise are usually met in the practice. Among them, the impulse noise is a kind of typical image noise, which including salt and pepper noise and random valued noise. Salt and pepper noise has a great impact on various image processing. For the salt and pepper noise denoising, the traditional filtering methods mainly include the linear mean filtering [14] and the non-linear median filtering [15]. At present, there are many methods have been developed to treat the salt and pepper noise. Fan *et al.* [16] regarded appearance of a noise point as a small probability event, and changed the noise point to be an objective or background pixel by replacing its gray level

with its neighborhood average gray level. Li and Xie [17] also regarded the appearance of a noise point as a small probability event, and segmented the noises from the edges and weak textures by using the improved two-dimensional Otsu algorithm, and constructed an adaptive fractional order function. Karthikeyan [18] proposed an efficient decision based algorithm for the removal of high density salt and pepper noise. For salt-and-pepper noise denoising, Nnolim [19] proposed an effective anisotropic diffusion mean filter which is robust to the impulse noise ranging from low to high density levels. Kannan [20] proposed an adaptive weighted fuzzy mean filter based on cloud model. Wang *et al.* [21] proposed a novel adaptive fuzzy switching weighted mean filter. In [22], a support vector machine classification based fuzzy filter is proposed. Lu *et al.* [23] proposed a novel three-values-weighted method. Deng *et al.* [24] presented an adaptive filtering method by using the multilayered pulse coupled neural network.

Since the traditional order of the fractional calculus is usually obtained by carrying out a large number of experiments, it can not achieve automatically and is not conducive to the practical application of the fractional calculus. In this paper, a fractional calculus operator for image denoising is constructed based on the characteristic of the local entropy and gradient feature, and an adaptive fractional calculus image denoising algorithm is proposed. Based on the quantitative assessment criteria of image denoising effect, such as peak signal to noise ratio(PSNR), information entropy(ENTROPY) and structural similarity index measurement (SSIM), the denoised performance is analyzed. The experimental results show that the proposed adaptive fractional calculus image denoising algorithm can not only preserve the image edges and texture, and image smoothing areas details while removing the noise, but also obtain a better visual effect.

The paper is organized as follows. In Section II, the construction of the fractional order denoising model is presented. In Section III, the realization of the adaptive fractional order calculus operator is described. In Section IV, the experimental results and their analysis is given. Finally, some conclusions are drawn in Section V.

II. FRACTIONAL ORDER DENOISING MODEL

For an arbitrary square integrable signal $f(t) \in L^2(R)$, its α order differential is represented as

$$D^{\alpha} f(t) = \frac{d^{\alpha} f(t)}{dt^{\alpha}}. \tag{1}$$

According to the basic theory of signal processing, its Fourier transform is defined as

$$\begin{aligned} D^{\alpha} f(t) \overset{FT}{\Leftrightarrow} (\hat{D}^{\alpha} f)(\omega) &= (i\omega)^{\alpha} \hat{f(\omega)} \\ &= |\omega|^{\alpha} \exp[i\theta^{\alpha}(\omega)] \hat{f(\omega)} \\ &= |\omega|^{\alpha} \exp[\frac{\alpha \pi i}{2} sgn(\omega)] \hat{f(\omega)}, \quad \alpha \in R, \end{aligned} \tag{2}$$

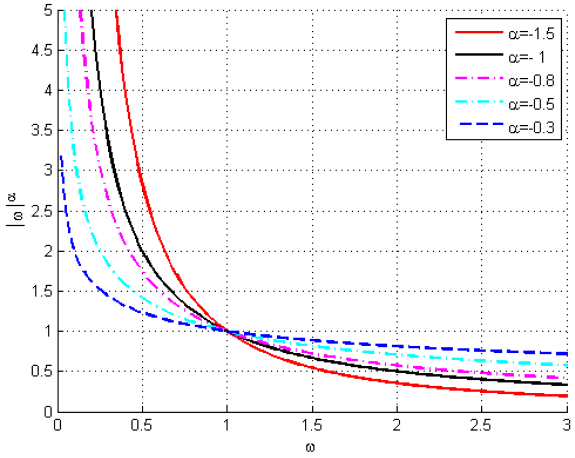

FIGURE 1. Amplitude-frequency characteristic curves of the fractional order integral.

where D^{α} is the differential operator with order α, ω is the angular frequency, $(i\omega)^{\alpha} = |\omega|^{\alpha} \exp[\frac{\alpha \pi i}{2} sgn(\omega)]$ is the filter function of fractional calculus filter, and $sgn(\cdot)$ represents the numeric symbol of the integer part. According to formula (2), we can draw the amplitude frequency characteristic curves with different fractional orders of ω as shown in Figure 1.

From Figure 1, it can be obviously seen that in the low frequency field with $0 < \omega < 1$, which corresponding to the image of the smooth regions, the fractional integral operator enlarges the amplitude values. However, in the intermediate frequency and high frequency part with $\omega > 1$, the fractional integral operator acts as an attenuation function, and the attenuation amplitude will be stronger as the fractional order or frequency increasing. This characteristic shows that the fractional integral operator can enhance the low frequency signal while attenuating the high frequency signal, and has a certain denoising effect on the noised images.

Taking into account the frequency characteristics of the fractional calculus, the calculus definition can be extended order from integer order to fraction order by using Gamma function $\Gamma(t)$. The fractional calculus formula with α-order of Grumwald-Letnikov(for short: G-L) definition [25], [26] is

$$D^{\alpha}_{G-L} f(t) = \lim_{h \to 0} h^{-\alpha} \sum_{k=0}^{[(t-a)/h]} (-1)^k \frac{\Gamma(\alpha+1)}{k!\Gamma(\alpha-k+1)} f(t-kh), \tag{3}$$

where $[\cdot]$ represents the integer portion, the duration of the signal $f(t)$ is $[a, t]$, α is an any real number (including fraction), D^{α}_{G-L} represents the fractional calculus operator defined by G-L, Γ is the Gamma function. When $\alpha > 0$, D^{α}_{G-L} is the fractional differential operator with α order, when $\alpha < 0$, D^{α}_{G-L} is the fractional integral operator with α order [13].

It is known that the shortest distance of grey intensity changes in a two-dimensional digital image is between its two adjacent pixels [27], so the duration time of a

two-dimensional digital image on the direction of x axis and y axis could only be measured in the pixel unit. Thus $h = 1$, then $n = [(t-a)/h] = [t-a]$. Therefore, according to G-L fractional calculus expression, we can get the differential expression with α order of signal $f(t)$ as:

$$D^{\alpha}_{G-L}f(t) \approx f(t) + (-\alpha)f(t-1) + \frac{(-\alpha)(-\alpha+1)}{2}f(t-2) + \ldots + \frac{\Gamma(-\alpha+1)}{k!\Gamma(-\alpha-k+1)}f(t-k). \quad (4)$$

For any function $f(x, y) \in L^2(R^2)$, the differential expressions for the partial calculus with α order with respect to x and y are as follows respectively:

$$\frac{d^{\alpha}f(x,y)}{dx^{\alpha}} \approx f(x,y) + (-\alpha)f(x-1,y) + \frac{(-\alpha)(-\alpha+1)}{2}f(x-2,y) + \cdots + \frac{\Gamma(-\alpha+1)}{k!\Gamma(-\alpha-k+1)}f(x-k,y), \quad (5)$$

$$\frac{d^{\alpha}f(x,y)}{dy^{\alpha}} \approx f(x,y) + (-\alpha)f(x,y-1) + \frac{(-\alpha)(-\alpha+1)}{2}f(x,y-2) + \cdots + \frac{\Gamma(-\alpha+1)}{k!\Gamma(-\alpha-k+1)}f(x,y-k). \quad (6)$$

With formulas (5) and (6), we can get a 5×5 fractional integral mask as shown in Figure 2. The mask is obtained by superimposing the partial fractional integral in eight directions, so it is rotation invariant. Where w_1, w_2 and w_3 are the first, second and third coefficient respectively of formulas (5) or (6), and $w_1 = 1$, $w_2 = -\alpha$ and $w_3 = (-\alpha)(-\alpha+1)/2$. In practice, the coefficients are divided by $8 - 12\alpha + 4\alpha^2$ for normalization. Now, we can get the image processed by α order fractional integral by considering airspace filtering of this mask convolution.

w_3	0	w_3	0	w_3
0	w_2	w_2	w_2	0
w_3	w_2	$8w_1$	w_2	w_3
0	w_2	w_2	w_2	0
w_3	0	w_3	0	w_3

FIGURE 2. Fractional integral mask.

III. IMPLEMENTATION OF THE ADAPTIVE FRACTIONAL CALCULUS OPERATOR

A. ANALYSIS OF IMAGE LOCAL FEATURES AFFECTED BY NOISE

1) GRADIENT

The gradient of an image reflects the spatial variation rate of the image. The gradient on the region with image edges and the texture rich is relatively large, and that on the regions with smoothing is small [28]. The gradient at pixel (x, y) of image $u_0(x, y)$ can be expressed as $G[u_0(x, y)] = [G'_x G'_y]^T = [\frac{\partial u_0}{\partial x} \frac{\partial u_0}{\partial y}]^T$. The formula of the gradient modulus is defined as

$$mag(G[u_0(x,y)]) = \sqrt{G'^2_x + G'^2_y}, \quad (7)$$

where $mag(\cdot)$ represents the gradient modulus,

$$G'_x = \Delta_x u_0(x,y) = u_0(x+1,y) - u_0(x,y),$$
$$G'_y = \Delta_y u_0(x,y) = u_0(x,y+1) - u_0(x,y).$$

In order to analyze the influence of noise on the gradient of an image, for the original image (a) and the noise image (b) shown as in Figure 3, we calculate their gradients and get the gradient image as shown in Figure 3(c) and Figure 3(d) respectively, where the density of the salt and pepper noise is set to be 0.03.

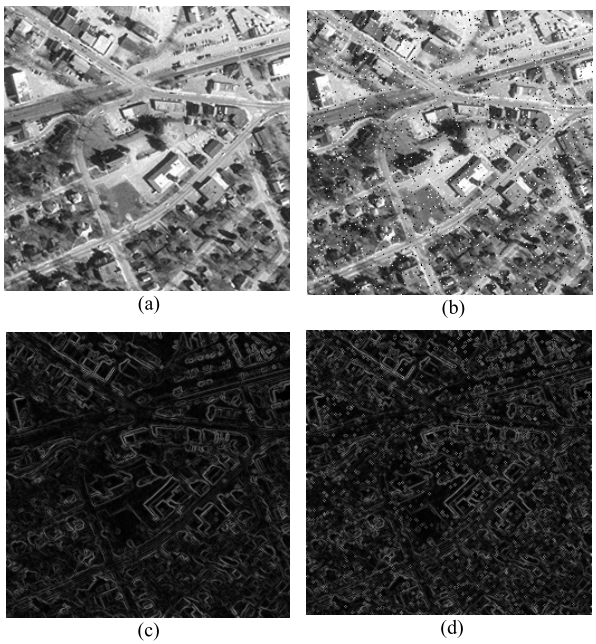

FIGURE 3. Gradient image. (a). Original image. (b). Noised image. (c). Gradient image of the original image. (d). Gradient image of the noised image.

From Figure 3(c) and Figure 3(d), we can see that the texture contours in the gradient image of the original image are clear, while the texture contours in the gradient image of the image with salt and pepper noise become blurred. It shows that the gradient of the image is greatly affected by noise. Taking into account the complexity of the pixel value range and more clearly showing the effect of noise on the gradient of the image, we use the area of 3×3 shown as in Figure 4 to further explain the influence of the noise.

Figure 5(a) shows the three-dimensional graph of the gradient of Figure 4(a) (in which the region is smooth), and Figure 5(b)shows that of Figure 4(b) with noise polluted.

From Figure 5(a), it can be seen that the change of the gradient value in the smooth region is relatively smooth.

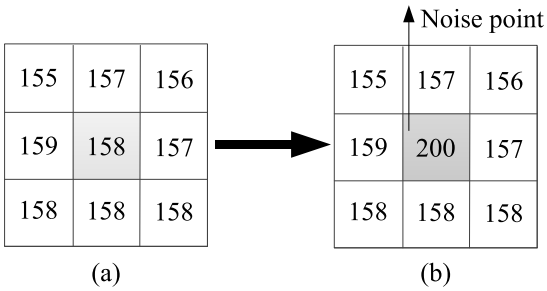

FIGURE 4. Current pixel and its neighbors. (a) Original pixels, (b) The center pixel has been blurred.

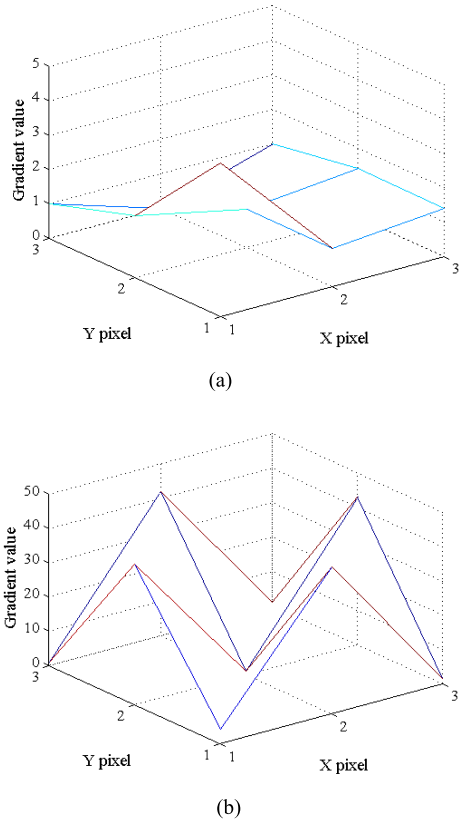

FIGURE 5. Three-dimensional graphs of gradient value. (a) Smooth region. (b) Noise region.

From Figure 5(b), it can be seen that the change of the gradient value of the noise polluted region is severe. In summary, we know that the image gradient value has a local mutation in the noise point, so it can be considered that the gradient value of the image is affected by the noise greatly. The stronger intense the noise is, the larger the gradient value is, and also the larger the attenuation amplitude of the image should be. Therefore, when doing denoising on a heavy noise point, the smaller (negative) the value of the adaptive operator should be taken to effectively suppress the image noise.

2) LOCAL ENTROPY

We know that the entropy plays an important role in the analysis of anomalous diffusion processes and fractional diffusion equations, some novel entropy indices and fractional operators are used to implement the complex dynamical systems [29], [30]. Entropy (ENTROPY) represents the probability of a particular information occurrence. The formula to calculate the entropy is defined as

$$H = -\sum_{g=0}^{255} p(g)\log_2 p(g), \tag{8}$$

where $p(g)$ is the probability of occurrence of the image gray value g, i.e. $p(g) = \frac{1}{s\times s}\sum_{u_0(x,y)=g} u_0(x,y)$, $g \in Z^+$, $(x,y) \in D_{local}$, D_{local} is the local region with size of $s \times s$, we take $s = 9$ in our experiments. Since the change of the grayscale value of the texture rich regions is larger than that of the smooth regions in the image, the value of entropy is relatively larger at the edges and the texture rich regions of the image.

In order to analyze the influence of noise on the local entropy of the image, we calculate the local entropy of the original image Figure 6(a) and the noise image Figure 6(b) respectively, and get the three-dimensional graphs as shown in Figure 6(c) and Figure 6(d), where the density of the salt and pepper noise is set to be 0.03.

Figure 6 (e) shows the histogram of residual error of the local entropy values between the original image and the noised image. Form Figure 6 (e), we can see that the difference value is mainly ranging on $-0.05\sim0.15$, so we can conclude that the noise points have a little effect on the local entropy value of the image. In summary, we know that the noise points have a little effect on the local entropy of the image, and the value of the local entropy can reflect the distribution of edges and texture regions in image. Therefore, the adaptive order used in the image denoiding should be constructed related to the local entropy of the image edges and texture regions. The larger the local entropy is, the richer the texture in the image is, the higher the order of the adaptive operator should be taken to enhance the boundaries and texture and to preserve more the texture detail information.

B. SEGMENT IMAGE COMBINED WITH SMALL PROBABILITY STRATEGY

Generally speaking, if we want to preserve or enhance the texture information of the image in the process of image denoising, we need to distinguish the noise points from the texture regions. We regard the appearance of the noise points in the image as a small probability event, and combine with the local structure to segment out the noise points, edges, texture regions and smooth regions.

Considering the pixel value range and the complexity of the local structure, we use a 3×3 region to analyze the image structure information as shown in Figure**7**, where P or P_i is the pixel.

The domain gray distance is defined as [31]:

$$D_i = I(P) - I(P_i), \quad i = 1, 2, \cdots, 8, \tag{9}$$

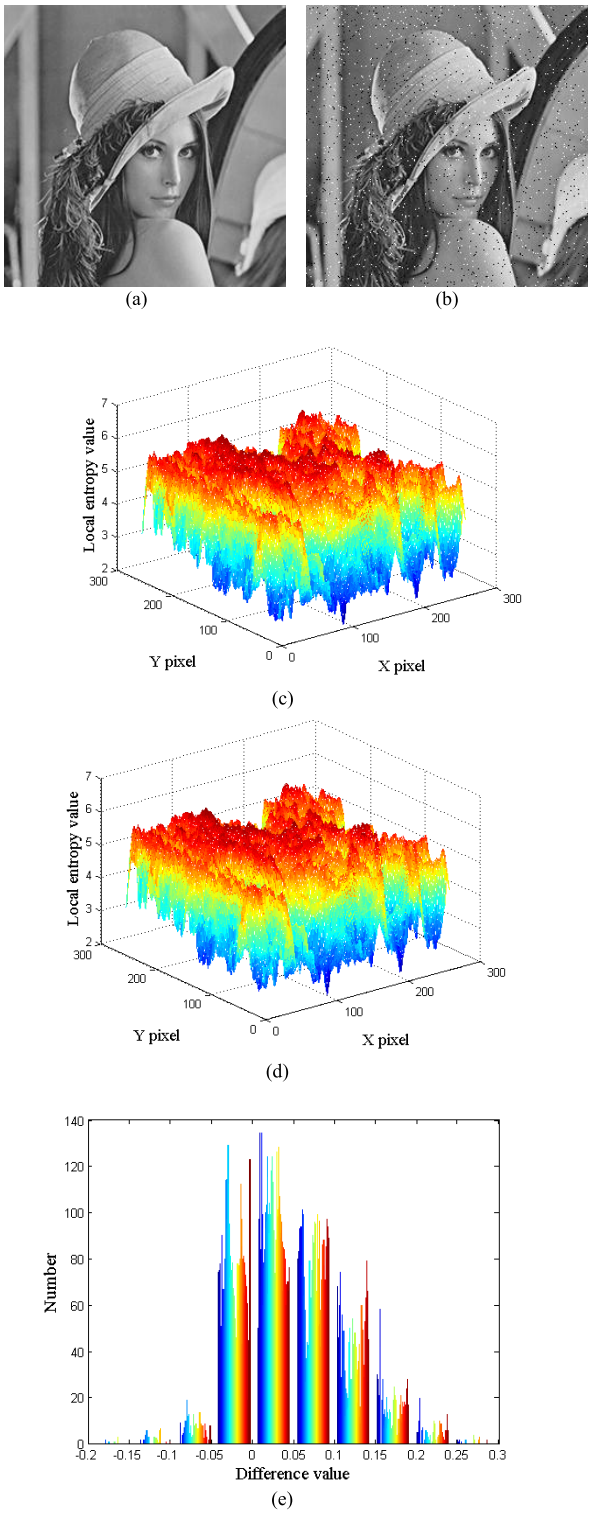

FIGURE 6. Local entropy. (a) Original image. (b) Noise image. (c) Local entropy of the original image. (d) Local entropy of the noise image. (e) Histogram of residual error.

where $I(P)$ is the gray value of pixel P. The minimum gray distance is:

$$D_{\min} = \min(D_i), \quad i = 1, 2, \cdots, 8. \tag{10}$$

P_1	P_2	P_3
P_4	P	P_5
P_6	P_7	P_8

FIGURE 7. Current pixel and its neighborhood.

The minimum absolute gray distance is:

$$AD_{\min} = \min(|D_i|). \tag{11}$$

According to the analysis of literature [17], we know that the gradient amplitudes of the image edges and noise points are relatively larger. But the edge pixels are mostly continuous, so the minimum absolute distance $AD_{\min}$ of the edge pixels in the eight directions are small. The noise points are generally random isolated points, so the minimum absolute distance $AD_{\min}$ in the eight directions are generally larger. For the noised image with low intensity salt and pepper noise, the occurrence of the noise points can be regarded as small probability events. Therefore, the minimum absolute distance $AD_{\min}$ of the pixels in the eight directions is arranged in descending order, and then the salt and pepper noise points can be segmented according to their probabilities.

Small probability event refers to the event that its occurrence is in an extremely small probability, this probability generally locates in the range of 0.01∼0.05 [16]. Assume that the occurrence of the noise point is a random event ξ, and the probability P_{noise} of occurrence of ξ is small, then for an image with size of $M \times N$, the mathematical expectation value of the number of noise points is

$$E = M \times N \times P_{noise}. \tag{12}$$

Arranging the value $AD_{\min}$ of all the pixel of the image in a descending order as $\{H(j)\}$, if $j \in [1, E]$, we determine the corresponding (P_x, P_y) is a noise point, i.e. the point (P_x, P_y) which satisfying formula (13) should be regarded as a noise point,

$$AD_{\min} \geq H(E). \tag{13}$$

Assume that the average value of the gray distance in each of the eight directions in the current pixel $u_0(x, y)$ is $M(x, y)$, then

$$M(x, y) = \frac{1}{8} \sum_{i=1}^{8} |D_i|. \tag{14}$$

Here, the minimum value $M(x, y)$ of the divided noise points is selected as the threshold value T of the image noise points. When $M(x, y) \geq T$, the corresponding pixel (x, y) is regarded as a noise point, and the larger the value of $M(x, y)$ is, the stronger of the noise is. Therefore, the amplitude of the gray should attenuate greatly when this pixel has been polluted by noise. When $1 < M(x, y) < T$, the corresponding

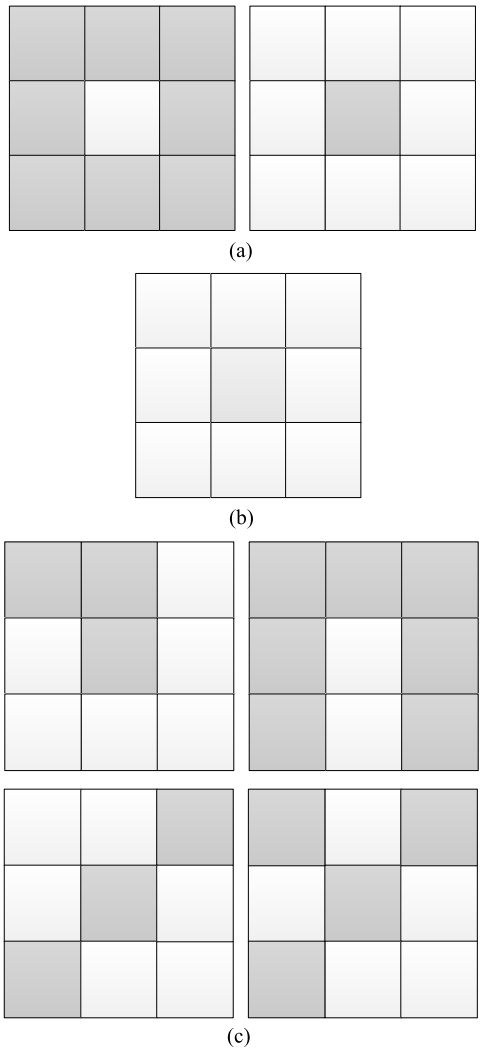

FIGURE 8. Examples of three basic types. (a) Isolated point. (b) Smooth regions. (c) Edges and texture regions.

pixel (x, y) is regarded as a point in the edges or texture regions, and it need to be enhanced in the denoising process. When $0 \leq M(x, y) \leq 1$, the pixel (x, y) is regarded as a point in the smooth regions, and the gray value of this pixel should remain unchanged during denoising. Figure 8 shows several examples of the three basic structure type pixels classified by local structure.

C. CONSTRUCTION OF ADAPTIVE FUNCTION

From Figure 1, we can see that the high frequency image noise can be effectively attenuated when the fractional differential order being taken as $\alpha \in [-1.5, -0.5]$, but it is too small to suppress noise satisfactorily. Therefore, for a pixel with different local characteristics such as the noise, edge and texture region, and smooth region, we should choose a different fractional order to do denoising to achieve a better effect.

From above analysis, it is known that the noise affects the gradient value, and the image edges and the texture regions

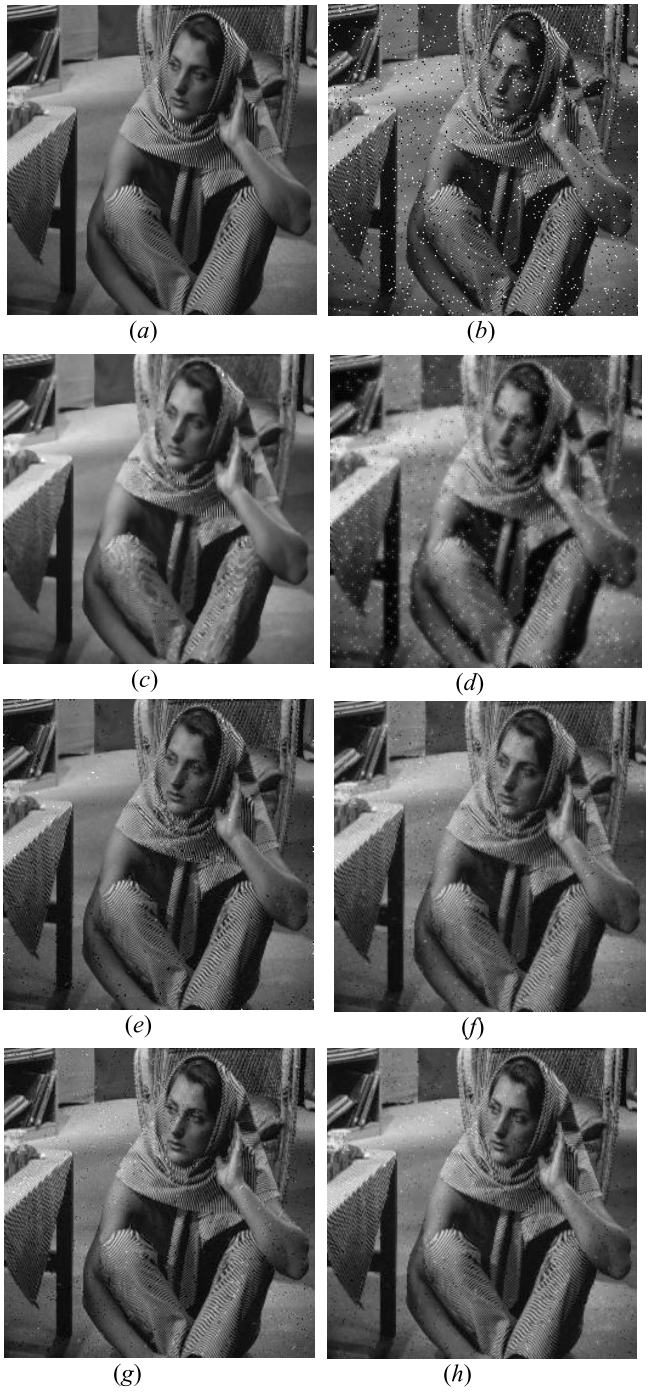

FIGURE 9. Denoising result images of noisy Barbara image with different types of algorithms. (a) Original image. (b) Noise image. (c) MF. (d) $\alpha = -1.1$. (e) SPS. (f) GAFIA. (g) AFC-SPS. (h) EN-AFC.

make the different value of the local entropy and gradient. Therefore, we will devote to find a function mapping between the fractional order α and the value of the local entropy and gradient of the image, to adaptively generate the order α depending on the local entropy and gradient. According to the characteristics of the different image regions, as formula (15) we construct an adaptive fractional order function respect to

FIGURE 10. Denoising result images of noisy Lena image with different types of algorithms. (a) Original image. (b) Noise image. (c) MF. (d) $\alpha = -1.1$. (e) SPS. (f) GAFIA. (g) AFC-SPS. (h) EN-AFC.

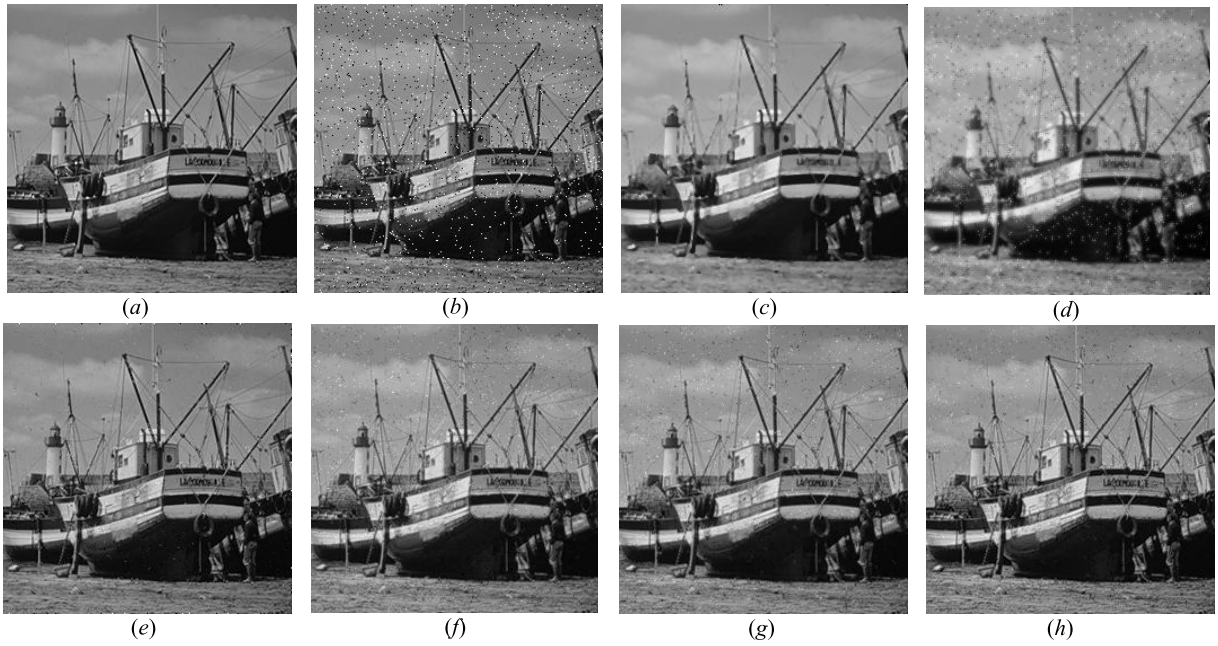

FIGURE 11. Denoising result images of noisy Boat image with different types of algorithms. (a) Original image. (b) Noise image. (c) MF. (d) $\alpha = -1.1$. (e) SPS. (f) GAFIA. (g) AFC-SPS. (h) EN-AFC.

the local entropy and gradient.

$$\alpha = \begin{cases} (-1.5) \times \dfrac{M(x,y) - T}{M_{\max} - M(x,y)}, & M(x,y) \geq T \\ \lambda_1 \times \dfrac{M(x,y)}{M_{\max}} + \lambda_2 \times \dfrac{EN(x,y) - meane}{\max e}, & 1 < M(x,y) < T \\ 0, & 0 \leq M(x,y) \leq 1, \end{cases} \tag{15}$$

where, $M(x, y)$ can be calculated by formula (14), $M_{\max}$ is the maximum value of $M(x, y)$, λ_1, λ_2 are the adjusting parameters, $EN(x, y)$ is the value of local entropy, *meane* is the mean of local entropy, $\max e$ is the maximum value of the local entropy, T is the threshold of the image noise points segmentation for the small probability strategy.

If $M(x, y)$ is larger than or equal to the noise points segmentation threshold T, then we can consider the corresponding pixel as a noised point. Therefore, the order should be taken as a negative value in the process of image denoising, and the value of the order is related to the value of $M(x, y)$. From the above analysis we can know that for a pixel, the larger the value of $M(x, y)$ is, the greater noise is, and the larger the attenuation amplitude is. Therefore the absolute value of the order is proportional to the value of $M(x, y)$. According to the experiment and analysis, we set the adaptive order for the corresponding noised point to be $\alpha = (-1.5) \times \frac{M(x,y)-T}{M_{\max}-M(x,y)}$. By selecting such an adaptive fractional order, if the noise is great, the value of the adaptive integral order (negative) will be small, and amplitude of the grey will be attenuated greatly.

If $M(x, y)$ is smaller than the segmentation threshold T but larger than 1, then the pixel can be regarded as a point in the image edges or texture regions. Therefore, in the process of image denoising, the fractional differential order should be taken as a positive value, and the value of the order is related to the value of $M(x, y)$ and $EN(x, y)$. From the above analysis we can conclude that if the value $EN(x, y)$ is large, the local area of the image will be a texture rich one, and the amplitude of the image should be enhanced when doing denoising. On the other hand, the noise points have little effect on the local entropy, so the value of the order is proportional to the value of $M(x, y)$ and $EN(x, y)$. According to the experiment and analysis, we construct the adaptive order for such points to be $\alpha = \lambda_1 \times \frac{M(x,y)}{M_{\max}} + \lambda_2 \times \frac{EN(x,y)-meane}{\max e}$.

According to the visual characteristics of the human eyes, we set the segmentation threshold for the image smooth regions to be 1. Therefore, if $M(x, y)$ is smaller than 1, then the pixel should be regarded as a point in the image smooth regions, and the gray value should remain unchanged in the process of image denoising.

IV. EXPERIMENTAL RESULTS AND ANALYSIS

In this section, the effectiveness of the proposed adaptive fractional order calculus denoising algorithm (EN-AFC) will be verified by comparing it with that of Median filtering [15] (MF), the traditional filter with order $\alpha = -1.1$, SPS [16], GAFIA [17], AFC-SPS [17]. In the SPS algorithm, the noise point is changed to be an objective or background pixel by using its neighborhood average gray value to instead its gray value. The GAFIA algorithm uses the fractional integral to process each pixel and finds the best order according to the global adaptive fractional function. In the AFC-SPS algorithm, the noise is divided based on that the appearance of the noise points are regarded as small probability events, and the image edges and weak textures are segmented by an improved two-dimensional Otsu algorithm. Thus they contructed a function of adaptive fractional order. The experimental simulation is run with software of MATLAB R2012a on a computer with 2.40GHz Intel Core i7 with 4GB RAM.

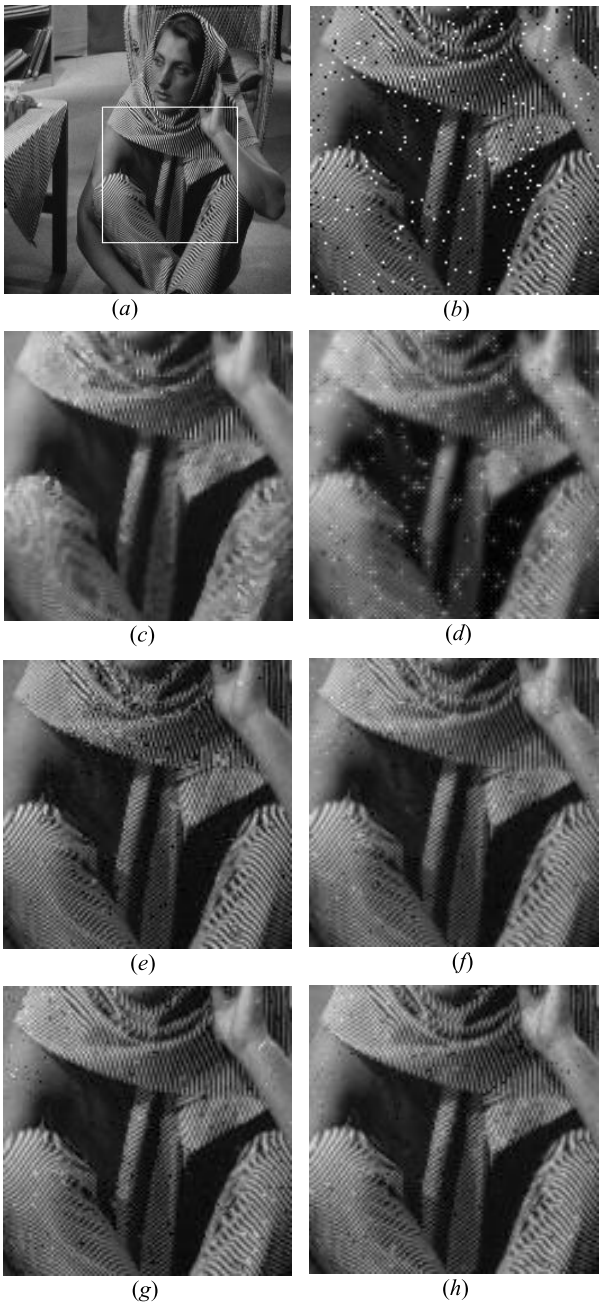

FIGURE 12. Local regions of denoising result images of noisy Barbara image with different types of algorithms. (a) Original image. (b) Noise image. (c) MF. (d) $\alpha = -1.1$. (e) SPS. (f) GAFIA. (g) AFC-SPS. (h) EN-AFC.

The images employed in the experiments are of size 256×256 with different textures, including Barbara image, Lena image, and Boat image. In this paper, we set $\lambda_1 = 0.4$, $\lambda_2 = 0.6$. As described above, small probability event generally locates in the range of 0.01∼0.05, so we take their average as the experimental noise intensity, which is the density of the salt and pepper noise set to be 0.03. The denoising results with EN-AFC, Median filtering, the traditional filter with order $\alpha = -1.1$, SPS, GAFIA, AFC-SPS on above three images are shown respectively as in Figure 9, Figure 10, Figure 11.

TABLE 1. Results of the PSNR of the denoised images with different types of algorithms.

Image	Noise image	MF[15]	$\alpha = -1.1$	SPS[16]	GAFIA[17]	AFC-SPS[17]	EN-AFC
Barbara	20.1768	23.1462	23.9714	28.3190	28.8119	29.0876	**29.6635**
Lena	20.9092	29.6595	25.7321	31.3508	30.9264	30.6697	**31.4666**
Boat	20.4231	27.0217	24.4234	30.6184	29.4851	29.6242	**30.6575**

TABLE 2. Results of the SSIM of the denoised images with different types of algorithms.

Image	Noise image	MF[15]	$\alpha = -1.1$	SPS[16]	GAFIA[17]	AFC-SPS[17]	EN-AFC
Barbara	0.6138	0.7154	0.6644	0.9129	0.8819	0.8790	**0.9027**
Lena	0.5779	0.9162	0.7148	0.9305	0.8790	0.8503	**0.8849**
Boat	0.5420	0.8703	0.6734	0.9425	0.8559	0.8608	**0.8924**

A. EVALUATION BY VISUAL EFFECTS

Here, we will evaluate the performance of image denoising algorithms by comparing their visual effects.

The best effect of image denoising is that the details of image boundaries and texture regions can be preserved while removing the image noise. From Figure 9 to Figure 11, we can see that Median filtering, SPS, GAFIA, AFC-SPS and EN-AFC can remove the image noise in a certain extent. Median filtering method almost eliminates all points of salt and pepper noise, but in the same time, it makes the edges and texture regions of the image blurred, and a lot of texture details information are lost, especially in Figure 9(c) and Figure 10(c), the textures are blurred seriously. The traditional order $\alpha = -1.1$ makes the image blurred, and makes the brightness of the image decreased at the same time. In order to further perform the advantage of our proposed method, in Figure 12 we present the denoising results of a small patch of the original noisy image.

From Figure 12(c), we can clearly see that Median filtering removes the noises, but makes the edges and texture regions blurred, and a lot of texture details information are lost. From Figure 12(e)–Figure 12(h), we can see that although the noises in the textures are not completely removed, but the edges and texture regions are clear. It shows that the algorithms can remove the noises and preserve the details information of the image edges and texture regions.

B. EVALUATION BY INDEXES

Here, different from section 4.1, we will objectively evaluate the performance of image denoising with quantitative evaluation indexes.

For an image denoising algorithm, its denoising effect can be evaluated with the peak signal to noise ratio (PSNR). The higher the value of PSNR is, the better the denoising effect of the algorithm is. PSNR is an engineering term that affects the fidelity of image representation [5]. It is the ratio of the maximum possible power of a signal to the destructive noise power and measured in decibels (dB). The peak signal to noise ratio is defined as:

$$MSE = \frac{1}{M \times N} \sum_{i=1}^{M} \sum_{j=1}^{N} [u_{\mathrm{n}}(i,j) - u_0(i,j)]^2, \quad (16)$$

$$PSNR = 10 \lg \frac{255^2}{MSE}, \quad (17)$$

where, the size of the original image is $M \times N$, $u_0(i,j)$ represents the original image, and $u_n(i,j)$ represents the denoised image. The comparison results of PSNR of four different algorithms are shown as in Table 1.

Structural similarity index measurement (SSIM) is mainly used to inspect the similarity between two images [32]. The higher the SSIM value is, the closer the image content is. Structural similarity index measurement is defined as:

$$SSIM = \frac{(2\mu_a\mu_b + c_1)(2\sigma_{ab} + c_2)}{(\mu_a^2 + \mu_b^2 + c_1)(\sigma_a^2 + \sigma_b^2 + c_2)}, \quad (18)$$

where a and b are two different images, μ_a and μ_b are the mean of a and b, respectively. σ_a^2 and σ_b^2 are the variance of a and b, respectively. σ_{ab} is the covariance of a and b, c_1, c_2 are constants used to maintain stability. The comparison results of SSIM of four different algorithms are shown as in Table 2, and of ENTROPY in Table 3.

We can carry on the objective evaluation for the image edges enhancement and image weak textures retention, by analyzing the peak signal to noise ratio, the structural similarity index measurement and the entropy of the denoised images. Form Figure 9(c) - Figure 11(c), we can see that Median filtering method can almost eliminate all of salt and pepper noises. However, from Table 3, we can see that the Median filtering obtains the lowest value of ENTROPY of the denoised image, which means that Median filtering makes the denoised image lost the details information. From Table 1 and Table 3, we can see that the values of PSNR of the denoised image with the SPS, GAFIA, AFC-SPS and the proposed adaptive denoising algorithm are higher, and the values of ENTROPY are also higher at the same time.

TABLE 3. Results of the ENTROPY of the denoised images with different types of algorithms.

Image	Original image	MF[15]	$\alpha = -1.1$	SPS[16]	GAFIA[17]	AFC-SPS[17]	EN-AFC
Barbara	7.3433	7.2681	7.2710	7.3474	7.3366	7.3732	**7.3649**
Lena	7.5132	7.4303	7.3859	7.5169	7.4865	7.5400	**7.5527**
Boat	7.1681	7.0660	7.1424	7.1786	7.1794	7.1918	**7.2035**

The values of PSNR and ENTROPY of the proposed adaptive denoising algorithm are slightly higher than that of the other compared algorithms. It shows that the proposed algorithm has a stronger ability to enhance the edges, the texture regions of the image, and preserve the smooth regions of the image while removing the noise.

V. CONCLUSIONS

In this paper, an image denoising algorithm based on entropy and adaptive fractional calculus is presented. In the proposed algorithm, the noise points are regarded as small probability events, and the noise points, edges, texture regions and smooth regions are segmented combined with the local structure. Thus a fractional order function is constructed with entropy and the gradient to improve the image denoising effect. With the comparison results, it can be seen that the proposed image denoising algorithm can effectively overcome the drawbacks of losing contrasting information and texture information. It can achieve improvement on keeping texture detailed image information, boundary information, and get a good visual effect, high values of PSNR and ENTROPY.

ACKNOWLEDGMENTS

The authors also thank sincerely the anonymous referee for his or her valuable comments, which helped in improving substantially the manuscript.

REFERENCES

[1] H. Jafari, H. K. Jassim, F. Tchier, and D. Baleanu, "On the approximate solutions of local fractional differential equations with local fractional operators," *Entropy*, vol. 18, no. 4, pp. 1–12, 2016.
[2] S. B. Zhou, X. R. Lin, and H. Li, "Chaotic synchronization of a fractional-order system based on washout filter control," *Commun. Nonlinear Sci. Numer. Simul.*, vol. 16, no. 3, pp. 1533–1540, 2011.
[3] Y. Wang, Y. Shao, Z. Gui, Q. Zhang, L. Yao, and Y. Liu, "A novel fractional-order differentiation model for low-dose CT image processing," *IEEE Access*, vol. 4, pp. 8487–8499, 2016.
[4] X. R. Lin, S. B. Zhou, and H. Li, "Chaos and synchronization in complex fractional-order Chua's system," *Int. J. Bifurcation Chaos.*, vol. 26, no. 3, p. 1650046, 2016.
[5] N. He *et al.*, "An improved fractional-order differentiation model for image denoising," *Signal Process.*, vol. 112, pp. 180–188, Sep. 2015.
[6] M. Srivastava, C. L. Anderson, and J. H. Freed, "A new wavelet denoising method for selecting decomposition levels and noise thresholds," *IEEE Access*, vol. 4, pp. 3862–3877, 2016.
[7] E. M. Eksioglu, "Decoupled algorithm for MRI reconstruction using nonlocal block matching model: BM3D-MRI," *J. Math. Imag. Vis.*, vol. 56, no. 3, pp. 430–440, 2016.
[8] G. Ghimpeteanu, T. Batard, and M. Bertalmío, "A decomposition framework for image denoising algorithms," *IEEE Trans. Image Process.*, vol. 25, no. 1, pp. 388–399, Jan. 2016.
[9] X. H. Yin, S. B. Zhou, and M. A. Siddique, "Fractional nonlinear anisotropic diffusion with p-Laplace variation method for image restoration," *Multimedia Tools Appl.*, vol. 75, no. 8, pp. 4505–4526, 2016.
[10] B. Li and W. Xie, "Adaptive fractional differential approach and its application to medical image enhancement," *Comput. Electr. Eng.*, vol. 45, pp. 324–335, Sep. 2015.
[11] L. P. Wang, S. B. Zhou, and A. Karim, "Super-resolution image reconstruction method using homotopy regularization," *Multimedia Tools Appl.*, vol. 75, no. 23, pp. 15993–16016, 2016.
[12] X. H. Yin and S. B Zhou, "Image structure-preserving denoising based on difference curvature driven fractional nonlinear diffusion," *Math. Problems Eng.*, vol. 2015, Apr. 2015, Art. no. 930984.
[13] Y.-F. Pu, J.-L. Zhou, and X. Yuan, "Fractional differential mask: A fractional differential-based approach for multiscale texture enhancement," *IEEE Trans. Image Process.*, vol. 19, no. 2, pp. 491–511, Feb. 2010.
[14] A. Kundu, S. Mitra, and P. Vaidyanathan, "Application of two-dimensional generalized mean filtering for removal of impulse noises from images," *IEEE Trans. Acoust., Speech, Signal Process.*, vol. 32, no. 3, pp. 600–609, Jun. 1984.
[15] B. I. Justusson, *Median Filtering: Statistical Properties*, vol. 43. Berlin, Germany: Springer, 1981, pp. 161–196.
[16] C. D. Fan, H. L. Ouyang, and Y. J. Zhang, "Small probability strategy based Otsu thresholding method for image segmentation," *J. Electron. Inf. Technol.*, vol. 35, no. 9, pp. 2081–2087, 2013.
[17] B. Li and W. Xie, "Image denoising and enhancement based on adaptive fractional calculus of small probability strategy," *Neurocomputing*, vol. 175, pp. 704–714, Sep. 2016.
[18] P. Karthikeyan, "Efficient decision based algorithm for the removal of high density salt and pepper noise in images," *J. Commun. Technol. Electron.*, vol. 61, no. 8, pp. 963–970, 2016.
[19] U. A. Nnolim, "Entropy-guided switching trimmed mean deviation-boosted anisotropic diffusion filter," *J. Electron. Imag.*, vol. 25, no. 4, p. 043001, 2016.
[20] K. Kannan, "An adaptive weighted fuzzy mean filter based on cloud model," *Int. Arab J. Inf. Technol.*, vol. 13, no. 6, pp. 609–613, 2016.
[21] Y. Wang *et al.*, "An efficient adaptive fuzzy switching weighted mean filter for salt-and-pepper noise removal," *IEEE Signal Process. Lett.*, vol. 23, no. 11, pp. 1582–1586, Nov. 2016.
[22] A. Roy *et al.*, "Impulse noise removal using SVM classification based fuzzy filter from gray scale images," *Signal Process.*, vol. 128, pp. 262–273, Sep. 2016.
[23] C. T. Lu *et al.*, "Removal of salt-and-pepper noise in corrupted image using three-values-weighted approach with variable-size window," *Pattern Recognit. Lett.*, vol. 80, pp. 188–199, Apr. 2016.
[24] X. Y. Deng, Y. D. Ma, and M. Dong, "A new adaptive filtering method for removing salt and pepper noise based on multilayered PCNN," *Pattern Recognit. Lett.*, vol. 79, pp. 8–17, Aug. 2016.
[25] K. B. Oldham and J. Spanier, "The fractional calculus," *Math. Gazette*, vol. 56, no. 247, pp. 396–400, 1974.
[26] E. R. Love, "Fractional derivatives of imaginary order," *J. London Math. Soc.*, vols. 2-3, no. 2, pp. 241–259, 1971.
[27] Y. F. Pu *et al.*, "Fractional differential approach to detecting textural features of digital image and its fractional differential filter implementation," *Sci. China Inf. Sci.*, vol. 51, no. 9, pp. 1319–1339, 2008.
[28] C. L. Wang, L. B. Lan, and S. B. Zhou, "Adaptive fractional differential and its application to image texture enhancement," *J. Chongqing Univ.*, vol. 34, no. 2, pp. 32–37, 2011.
[29] C. Ingo, R. L. Magin, and T. B. Parrish, "New insights into the fractional order diffusion equation using entropy and kurtosis," *Entropy*, vol. 16, no. 11, pp. 5838–5852, 2014.
[30] L. I. Karmele *et al.*, "Symmetric fractional diffusion and entropy production," *Entropy*, vol. 18, no. 8, p. 275, 2016.

[31] Z. M. Wang and L. Zhang, "Local-structure-adapted image diffusion," *Acta Autom. Sinica*, vol. 35, no. 3, pp. 244–250, 2009.
[32] Z. Wang, A. C. Bovik, H. R. Sheikh, and E. P. Simoncelli, "Image quality assessment: From error visibility to structural similarity," *IEEE Trans. Image Process.*, vol. 13, no. 4, pp. 600–612, Apr. 2004.

JIMIN YU received the Ph.D. degree in applied mathematics from Zhengzhou University in 2003. He is currently a Professor with the Key Laboratory of Industrial Wireless Networks and Networked Control, Ministry of Education, and the College of Automation, Chongqing University of Posts and Telecommunications. His research interests include fractional order dynamic systems, numerical methods, and stability theory of functional equations.

LIJIAN TAN received the B.S. degree in mechanical electrical engineering from Hubei University for Nationalities, China, in 2014. He is currently pursuing the M.S. degree in control engineering with the Chongqing University of Posts and Telecommunications. His research interests include image restoration and probe automatic positioning.

SHANGBO ZHOU received the B.Sc. degree in mathematics from the Gangxi National College in 1985, the M.Sc. degree in mathematics from Sichuan University in 1991, and the Ph.D. degree in circuit and system from Electronic Science and Technology University. From 1991 to 2000, he was with the Chongqing Aerospace Electronic and Mechanical Technology Design Research Institute. Since 2003, he has been with the College of Computer Science and Engineering, Chongqing University, where he is currently a Professor. His current research interests include artificial neural networks, physical engineering simulation, image processing, and nonlinear dynamics.

LIPING WANG received the B.Sc. degree in information management and information system from Zhengzhou University, Zhengzhou, China, in 2004, the master's degree in technology of computer application from the Chongqing University of Posts and Telecommunications, Chongqing, in 2010. He is currently pursuing the Ph.D. degree with the College of Computer Science, Chongqing University. He was a Teacher with the College of Shengda Economics Trade and Management, Zhengzhou University, from 2004 to 2007. His research interests include image restoration, pattern recognition, and inverse problems.

MUHAMMAD ABUBAKAR SIDDIQUE received the B.Sc. degree in computer science and the master in information technology (MIT) degree from Bahauddin Zakariya University, Multan, Pakistan, in 2003 and 2005, respectively, and the Ph.D. degree from the College of Computer Science, Chongqing University, China, in 2015. He is currently working as Assistant Professor in Khwaja Fareed University of Engineering & Information Technology, Rahim Yar Khan-Pakistan. His research interests include multimedia mining and pattern recognition.